PROCEEDINGS OF SCIENCE

Measurement of leading neutron production in DIS at HERA

Armen Bunyatyan[*†]
DESY, Notkestrasse 85, 22603 Hamburg, Germany
E-mail: Armen.Bunyatyan@desy.de

The production of leading neutrons, where the neutron carries a large fraction x_L of the incoming proton's longitudinal momentum, is studied in deep-inelastic positron-proton scattering at HERA. The data were taken with the H1 detector in the years 2006 and 2007 and correspond to an integrated luminosity of 122 pb^{-1}. The semi-inclusive cross section is measured in the phase space defined by the photon virtuality $6 < Q^2 < 100$ GeV^2, Bjorken scaling variable $1.5 \cdot 10^{-4} < x < 3 \cdot 10^{-2}$, longitudinal momentum fraction $0.32 < x_L < 0.95$ and neutron transverse momentum $p_T < 0.2$ GeV. The leading neutron structure function, $F_2^{LN(3)}(Q^2, x, x_L)$, and the fraction of deep-inelastic scattering events containing a leading neutron are studied as a function of Q^2, x and x_L. Assuming that the pion exchange mechanism dominates leading neutron production, the data provide constraints on the shape of the pion structure function.

XVIII International Workshop on Deep-Inelastic Scattering and Related Subjects
April 19 -23, 2010
Convitto della Calza, Firenze, Italy

[*]Speaker.
[†]On behalf of the H1 Collaboration

PoS(DIS 2010)062

1. Introduction

Events containing a neutron, which carries a large fraction x_L of the longitudinal momentum of the incoming proton, have been observed in ep collisions at HERA [1, 2]. These leading neutrons (LN) can be produced in the fragmentation of the proton remnant, as illustrated in Fig. 1a. However, the exchange of a virtual pion (Fig. 1b) dominates LN production at large x_L and low transverse momentum of the neutron [3-8]. In this picture the proton fluctuates into a state consisting of a π^+ and a neutron. The virtual photon subsequently interacts with a parton from the pion. Consequently, the cross section factorises into a factor describing the $p \to n\pi^+$ fluctuation and a factor describing the photon-pion scattering (proton vertex factorisation). The production of LN in DIS at HERA therefore provides constraints on the pion structure at low to medium Bjorken $-x$, while the knowledge of the pion structure from fixed target experiments is limited to higher x values.

Here a new measurement of the semi-inclusive cross section for leading neutron production in DIS is presented [9]. The data used in this analysis were collected with the H1 detector at HERA in the years 2006 and 2007 and correspond to an integrated luminosity of 122 pb^{-1}. The dataset, which is 36 times larger than that used in the previous H1 publication [1] together with better experimental capabilities allow the extension of the kinematic range of the measurement to higher values of x and the virtuality of the exchanged photon Q^2 and the reduction of the total uncertainty of the results.

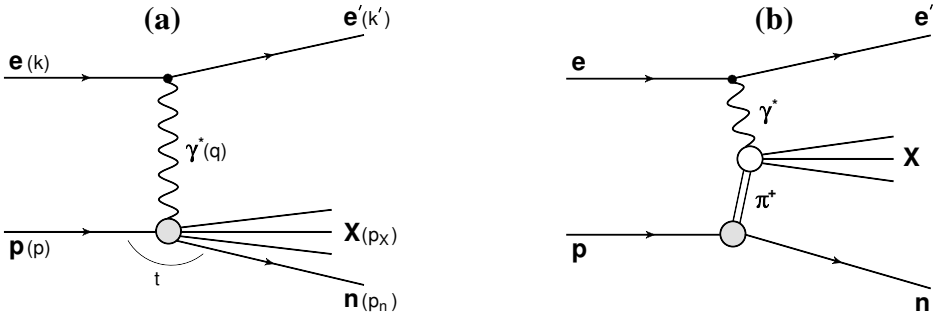

Figure 1: (a) Generic diagram for leading neutron production $ep \to e'nX$ in deep-inelastic scattering. (b) Diagram of the same process assuming that it proceeds via pion exchange.

2. Event kinematics and Data analysis

The kinematic variables used to describe the inclusive DIS scattering process are defined as

$$Q^2 = -q^2\,, \qquad x = Q^2/(2p\cdot q)\,, \qquad y = (p\cdot q)/(p\cdot k)\,, \tag{2.1}$$

where p, k and q are the four-momenta of the incident proton, the incident positron and the exchanged virtual photon, respectively (see Fig. 1a). The kinematic variables x_L and the squared four-momentum transfer t are used to describe the final state neutron

$$x_L = 1 - \frac{q\cdot(p-p_n)}{q\cdot p} \simeq E_n/E_p, \qquad t = (p-p_n)^2 \simeq -\frac{p_T^2}{x_L} - (1-x_L)\left(\frac{m_n^2}{x_L} - m_p^2\right), \tag{2.2}$$

where m_p is the proton mass, p_n is the four-momentum of the final state neutron, m_n is the neutron mass and E_n and p_T are the neutron energy and transverse momentum, respectively.

The DIS events are selected within the kinematic range $6 < Q^2 < 100$ GeV^2, $0.02 < y < 0.6$ and $1.5 \cdot 10^{-4} < x < 3 \cdot 10^{-2}$. Leading neutrons are detected in the forward neutron calorimeter, which is situated at 106 m from the interaction point at a polar angle of 0°. Events are selected containing a neutron with a polar angle below 0.75 mrad, $x_L > 0.3$ and $p_T < 0.2$ GeV. The final data sample contains 209150 events.

In this analysis the DJANGO [10] program is used for the generation of standard DIS events, where leading neutrons originate from proton remnant fragmentation. Leading neutron production via pion exchange is simulated by the RAPGAP [11] generator (RAPGAP-π). The pion flux factor associated with the splitting of a proton into a $\pi^+ n$ system is taken from [5] as

$$f_{\pi^+/p}(x_L,t) = \frac{1}{2\pi}\frac{g^2_{p\pi n}}{4\pi}(1-x_L)\frac{-t}{(m_\pi^2-t)^2}\exp\left(-R^2_{\pi n}\frac{m_\pi^2-t}{1-x_L}\right), \tag{2.3}$$

where m_π is the pion mass, $g^2_{p\pi n}/4\pi = 13.6$ and $R_{\pi n} = 0.93$ GeV^{-1}.

3. Results

The differential cross section of LN production as a function of x_L is presented in the left side of Fig. 2. The distribution is well described by the combination of the RAPGAP-π and DJANGO simulations using some global weighting factors. For large values of x_L, the shape of the distribution is well described by RAPGAP-π. This indicates that the π-exchange mechanism dominates at high x_L, while proton remnant fragmentation gives a significant contribution at low x_L.

The right side of Fig. 2 presents the measurement of the semi-inclusive structure function $F_2^{LN(3)}(Q^2,x,x_L)$, defined by:

$$\frac{\mathrm{d}^3\sigma(ep\to enX)}{\mathrm{d}x\,\mathrm{d}Q^2\,\mathrm{d}x_L} = \frac{4\pi\alpha^2}{xQ^4}\left(1-y+\frac{y^2}{2}\right)F_2^{LN(3)}(Q^2,x,x_L). \tag{3.1}$$

In all (Q^2,x) bins the distributions are reasonably well described by the combination of RAPGAP-π and DJANGO simulations.

The measurement of $F_2^{LN(3)}$ allows the validity of the hypothesis of limiting fragmentation [13, 14] to be tested, which implies that LN production in DIS is insensitive to x and Q^2. To investigate this prediction, the ratio of $F_2^{LN(3)}$ to the proton structure function F_2 is studied as a function of Q^2 in bins of x and x_L (Fig. 3 (left)). These average values decrease from 7% to 2% with increasing x_L. The ratios are almost independent of x and Q^2 in each x_L bin, implying that $F_2^{LN(3)}$ and F_2 have a similar (Q^2,x) behaviour, as expected from the hypothesis of limiting fragmentation.

Assuming that leading neutrons are produced via the exchange of a colour singlet particle, the structure function $F_2^{LN(3)}$ factorises into a flux factor which is a function of x_L and a structure function $F_2^{LN(2)}$ which depends on Q^2 and $\beta = x/(1-x_L)$. The quantity β can be interpreted as the fraction of the exchanged particle's momentum carried by the parton interacting with the virtual photon. The distribution of $F_2^{LN(3)}$, shown in Fig. 3 (right), has a similar dependence on β in all (Q^2,x_L) bins which can be approximated and fitted by a power law function $\propto \beta^{-\lambda}$. Within uncertainties the value of the fitted parameter λ is independent of x_L which is consistent with proton vertex factorisation.

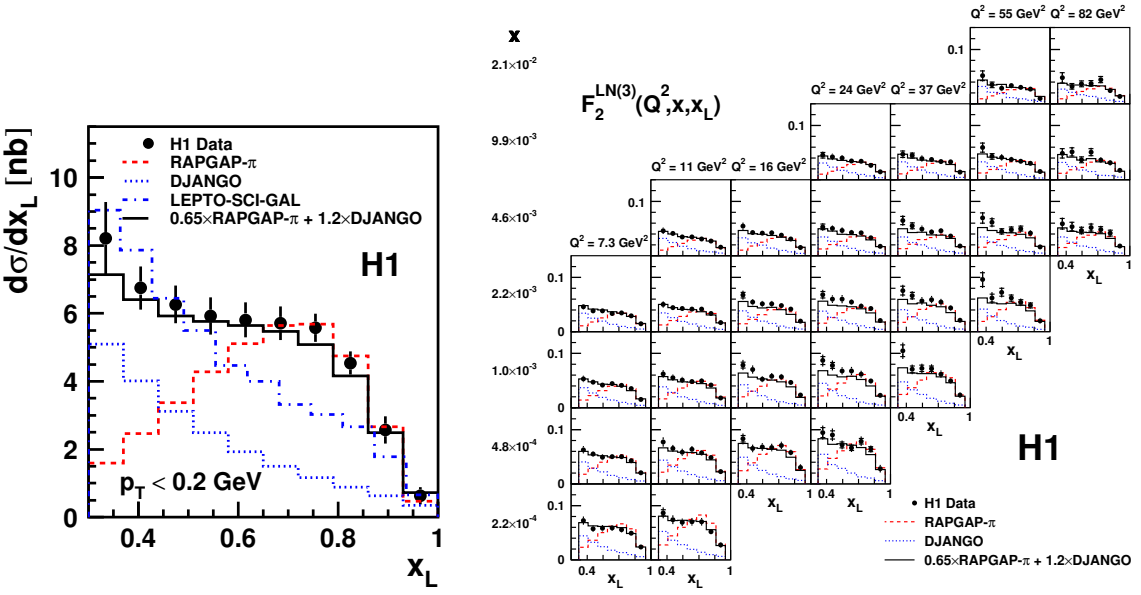

Figure 2: (left) The cross section as a function of the fractional energy of the neutron x_L in the kinematic range $6 < Q^2 < 100$ GeV^2, $1.5 \cdot 10^{-4} < x < 3 \cdot 10^{-2}$, $0.02 < y < 0.6$ and $p_T < 0.2$ GeV. The data are compared to the predictions of RAPGAP-π, DJANGO and LEPTO-SCI-GAL [12] Monte Carlo simulations. (right) The semi-inclusive structure function $F_2^{LN(3)}(Q^2,x,x_L)$ compared to the Monte Carlo models.

Since pion exchange dominates leading neutron production at high x_L and low p_T, the measurement of $F_2^{LN(3)}$ in the range $0.68 < x_L < 0.77$ can be used to estimate the pion structure function at low Bjorken-x. Assuming proton vertex factorisation the quantity $F_2^{LN(3)}/\Gamma_\pi$ can be interpreted as being equal to the structure function of the pion, where $\Gamma_\pi(x_L)$ is the integral of the pion flux over the measured t-range. The pion flux from Eq. 2.3 used for the RAPGAP-π simulation yields $\Gamma_\pi = 0.13$ for $p_T^{\max} = 0.2$ GeV at $x_L = 0.73$, which is the central value of the chosen x_L range. Using other parameterisations of the pion flux leads to values of the pion flux integral which may differ by up to 30%. In this evaluation of the pion structure function contributions from background processes like the exchange of ρ and a_2-mesons, proton diffractive dissociation and Δ production are not taken into account. Within the narrow x_L range considered here they are only expected to affect the absolute normalisation of the results. The normalisation the pion flux factor may depend also on absorptive corrections which are not taken into account in this analysis.

Figure 4 shows $F_2^{LN(3)}/\Gamma_\pi$ as a function of Q^2 in bins of β and as a function of β in bins of Q^2. The measurements are compared to the parameterisations of the pion structure function GRSc-π [16] and ABFKW-π [17] and to the H1PDF2009 parameterisation of the proton structure function $F_2(Q^2,x)$ [15] which is scaled by a factor of 2/3 in order to account for the different number of valence quarks in the pion and proton, respectively. The Q^2 distribution exhibits a rise with increasing Q^2 (i.e. scaling violation) for all β values in the measured range, which is similar in size and shape to that seen in the parameterisations of the inclusive structure functions of both the pion and proton. The β distributions show a steep rise with decreasing β for all Q^2 values. This behaviour is in reasonable agreement with the pion and proton structure function parameterisations.

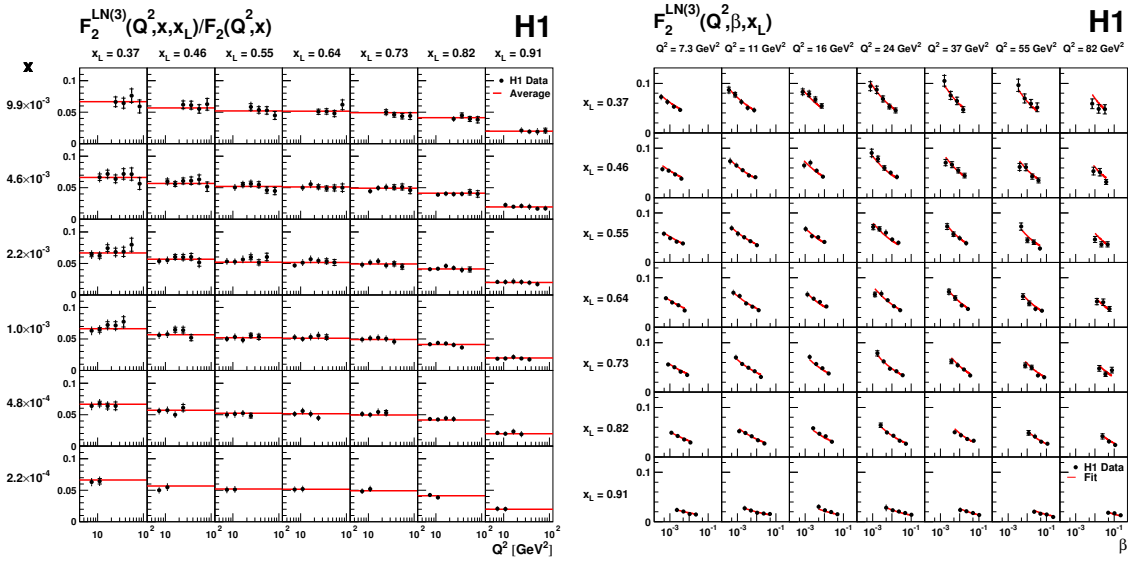

Figure 3: (left) The ratio of the semi-inclusive structure function $F_2^{LN(3)}(Q^2,x,x_L)$ to the proton structure function $F_2(Q^2,x)$ obtained from the H1PDF2009 fit to inclusive DIS data [15]. The lines show the average value for a given x_L bin. (right) The semi-inclusive structure function $F_2^{LN(3)}(Q^2,\beta,x_L)$ shown as a function of β in bins of Q^2 and x_L. The lines are the results of the fit with a function $c(x_L)\cdot\beta^{-\lambda(Q^2)}$.

4. Summary

The cross section for leading neutron production in deep-inelastic positron-proton scattering $d\sigma/dx_L$ and the semi-inclusive structure function $F_2^{LN(3)}(Q^2,x,x_L)$ are measured in the kinematic region $6 < Q^2 < 100$ GeV^2, $1.5\cdot10^{-4} < x < 3\cdot10^{-2}$, $0.32 < x_L < 0.95$ and $p_T < 0.2$ GeV.

The measurements are well described by a Monte Carlo simulation including neutron production in fragmentation and neutrons produced from π^+ exchange. Within the measured kinematic range, the semi-inclusive structure function $F_2^{LN(3)}$ and the inclusive structure function F_2 have similar (Q^2,x) behaviour. The dependence of $F_2^{LN(3)}$ on the variable β is similar for all x_L bins, in accordance with the proton vertex factorisation hypothesis. The scaling violations observed in $F_2^{LN(3)}$ are similar in size and shape to those seen in the parameterisations of the inclusive structure functions of the pion and the proton. The data are used to estimate the structure function of the pion.

References

[1] C. Adloff *et al.* [H1 Collaboration], Eur. Phys. J. C **6** (1999) 587 [hep-ex/9811013].

[2] S. Chekanov *et al.* [ZEUS Collaboration], Nucl. Phys. B **637** (2002) 3 [hep-ex/0205076].

[3] J.D. Sullivan, Phys. Rev. D **5** (1972) 1732.

[4] M. Bishari, Phys. Lett. B **38** (1972) 510.

[5] H. Holtmann *et al.*, Phys. Lett. B **338** (1994) 363.

[6] B. Kopeliovich, B. Povh and I. Potashnikova, Z. Phys. C **73** (1996) 125 [hep-ph/9601291].

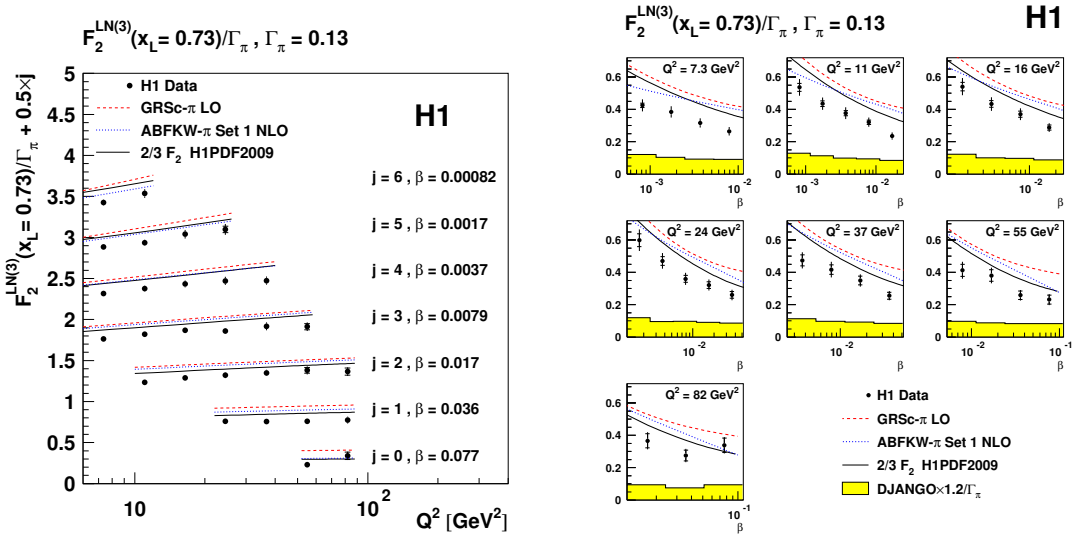

Figure 4: The semi-inclusive structure function $F_2^{LN(3)}$ divided by the pion flux Γ_π integrated over t at the central value $x_L = 0.73$, shown as a function of Q^2 in bins of β and as a function of β in bins of Q^2 The data are compared to two parameterisations of the pion structure function F_2^π and to the H1PDF2009 parameterisation of the proton structure function which has been scaled by 2/3.

[7] A. Szczurek, N.N. Nikolaev and J. Speth, Phys. Lett. B **428** 383 (1998) 383 [hep-ph/9712261].

[8] V.A. Khoze, A.D. Martin and M.G. Ryskin, Eur. Phys. J. C **48** (2006) 797 [hep-ph/0606213].

[9] F.D. Aaron *et al.* [H1 Collaboration], DESY-09-185, submitted to Eur. Phys. J. C. [arXiv:1001.0532].

[10] K. Charchula, G. Schuler and H. Spiesberger, DJANGOH 1.4, Comp. Phys. Commun. **81** (1994) 381.

[11] H. Jung, RAPGAP 3.1, Comp. Phys. Commun. **86** (1995) 147.

[12] A. Edin, G. Ingelman and J. Rathsman, Phys. Lett. B **366** (1996) 371 [hep-ph/9508386].

[13] J. Benecke *et al.*, Phys. Rev. **188** (1969) 2159.

[14] T.T. Chou and C.-N. Yang, Phys. Rev. D **50** (1994) 590.

[15] F.D. Aaron *et al.* [H1 Collaboration], Eur. Phys. J. C **64** (2009) 561 [arXiv:0904.3513.].

[16] M. Glück, E. Reya and I. Schienbein, Eur. Phys. J. C **10** (1999) 313 [hep-ph/9903288].

[17] P. Aurenche *et al.*, Phys. Lett. B **233** (1989) 517.